J. Physiol. (1962), **160**, *pp.* 317–352
With 15 *text-figures*
Printed in Great Britain

A MODIFICATION OF THE HODGKIN–HUXLEY EQUATIONS APPLICABLE TO PURKINJE FIBRE ACTION AND PACE-MAKER POTENTIALS

BY D. NOBLE

From the Department of Physiology, University College London

(*Received* 19 *July* 1961)

In 1949 Hodgkin & Katz showed that the amplitude and rate of rise of the action potential of squid nerve vary with the extracellular sodium concentration in a way which suggested that the rising phase of the nerve impulse is produced by a large and specific increase in the permeability of the membrane to sodium ions. Since the sodium equilibrium potential is normally opposite in sign to that of potassium, this hypothesis readily accounted for the reversal of the membrane potential which had already been observed (Hodgkin & Huxley, 1939, 1945; Curtis & Cole, 1940, 1942).

Using the voltage-clamp technique, Hodgkin & Huxley (1952*a*, *b*, *c*, *d*) separated the membrane current into sodium and potassium components and formulated equations describing the way in which these currents vary with membrane potential and time. They showed that, when combined with the equations of cable theory, their equations could accurately reproduce many of the electrical properties of squid nerve including the shape and size of the action potential, impedance changes, velocity of conduction and the ionic exchanges. The range of phenomena to which they have been shown to apply has since been greatly extended. The original hand computations were confirmed by Cole, Antosiewicz & Rabinowitz (1955) who first set the equations up on an electronic computer. Huxley (1959*a*) has applied the equations to the influence of temperature on the propagated response and to the repetitive firing observed in low calcium concentrations, using the experimental information obtained by Frankenhaeuser & Hodgkin (1957). The prolonged action potentials produced by treating squid nerve with tetraethylammonium ions (Tasaki & Hagiwara, 1957) may be largely accounted for by greatly slowing the rise in potassium permeability (Fitzhugh, 1960; George & Johnson, 1961) and the hyperpolarizing responses obtained at high extracellular potassium concentrations (Segal, 1958; Tasaki, 1959) may be described, at least qualitatively, by introducing the appropriate change in the potassium equilibrium potential (Moore, 1959; George & Johnson, 1961).

The aim of the computations described in this paper is to test whether, with certain modifications, Hodgkin & Huxley's formulation of the properties of excitable membranes may also be used to describe the long-lasting action and pace-maker potentials of the Purkinje fibres of the heart. These fibres differ from squid nerve in that depolarization *decreases* the potassium permeability of the membrane (Hutter & Noble, 1960; Carmeliet, 1961). During large depolarizations part of this decrease appears to be only transient and the potassium permeability slowly increases during the passage of the depolarizing current (Hutter & Noble, 1960). The equations describing the dependence of the potassium current on potential and time have been modified to take account of this behaviour. The sodium current equations, however, are very similar to those of Hodgkin & Huxley and are in part based on Weidman's (1955) voltage-clamp experiments. The solution to these equations closely resembles the Purkinje fibre action and pace-maker potentials and it will be shown that its behaviour in response to 'applied currents' and to changes in 'ionic permeability' corresponds fairly well with that observed experimentally.

Preliminary reports of some of this work have already been published (Noble, 1960*a*, *b*). The defect in the potassium current equations then used has now been corrected and this change accounts for the small quantitative differences between the conductance changes described in this paper and previously.

DESCRIPTION OF THE MEMBRANE CURRENT IN PURKINJE FIBRES

The basic feature of Hodgkin & Huxley's (1952*d*) formulation of the properties of excitable membranes is that the current is carried by ions moving down their respective electrochemical potential gradients. The sodium current, for example, changes direction when the sodium electrochemical potential gradient is reversed, by changing either the membrane potential or the extracellular sodium concentration (Hodgkin & Huxley, 1952*a*). In cardiac muscle this point has not been directly tested, since it has not yet proved possible to apply the voltage-clamp technique in its original form. The possibility that current is also produced by an electrogenic pump cannot therefore be entirely excluded. However, there is no conclusive experimental evidence for this view and in this paper it will be assumed that none of the membrane current is of direct metabolic origin. On this view the current carried by an ion species depends only on the magnitude of its electrochemical potential gradient and on the ease with which the ions may cross the cell membrane.

Hodgkin & Huxley (1952*a*) showed that for squid nerve in sea water the permeability of the membrane to Na and K ions is best described in terms of the contributions which these ions make to the membrane

conductance. The individual ionic conductances are defined by the equations

$$g_{Na} = I_{Na}/(E_m - E_{Na}), \quad (1)$$

$$g_K = I_K/(E_m - E_K), \quad (2)$$

where g_{Na} and g_K are the sodium and potassium conductances respectively in mmho/cm^2,

I_{Na} and I_K are the ionic currents in μA/cm^2,

E_{Na} and E_K are the equilibrium potentials in mV

and E_m is the membrane potential in mV expressed as the inside potential minus the outside potential.

In addition, a leak conductance was assumed which may be attributed, at least in part, to chloride ions. It will be convenient in this paper to refer to this as the anion conductance, g_{An}

$$g_{An} = I_{An}/(E_m - E_{An}), \quad (3)$$

where I_{An} is the anion current and E_{An} the anion equilibrium potential. Various values for g_{An} will be inserted in order to reproduce the effects of anions of different permeabilities.

In Hodgkin & Huxley's equations the membrane potential (V) is measured with respect to a 'zero' at the resting potential and has a sign such that the action potential is a negative variation in V. The convention adopted here is different and conforms to that usually adopted in experimental work with intracellular electrodes. The potential (E_m) is the potential of the inside with respect to the outside, the resting potential is a negative quantity and the action potential is a positive variation. Positive currents are therefore outward and not inward as in Hodgkin & Huxley's equations. In comparing the equations in this paper with those of Hodgkin & Huxley the substitution $E_m = E_r - V$ should be made, where E_r is the resting potential of squid nerve (about -55 mV).

The total membrane current (I_m) is given by the sum of the ionic currents and the current flowing into the membrane capacity

$$I_m = C_m \frac{dE_m}{dt} + I_{Na} + I_K + I_{An}, \quad (4)$$

where C_m is the membrane capacity and t is time in msec. C_m will be taken to be 12μF/cm^2 (Weidmann, 1952; Coraboeuf & Weidmann, 1954) which is 12 times larger than in squid nerve. If an action potential is initiated at all points along a fibre simultaneously, the membrane potential at each instant will be uniform. The axial current will therefore be zero, so that, in the absence of applied currents, the total membrane current will also be zero. This type of response was called a 'membrane' action potential by Hodgkin & Huxley and is given by equation (4) with $I_m = 0$. In these circumstances all the net ionic current is used in changing the charge on the local membrane capacity, so that the rate of change of potential, dE_m/dt,

is proportional to the net ionic current. In the present paper only membrane action potentials will be described and in comparing the results with experimental records of propagated action potentials it is assumed that the axial current, which must be very small during the slow phases of the action potential, may be neglected.

The equivalent electrical circuit assumed for the Purkinje fibre membrane is shown in Fig. 1. The only qualitative difference between this and the circuit for squid nerve (Hodgkin & Huxley, 1952*d*) is that the potassium current is assumed to flow through two non-linear resistances. The reason for making this assumption is explained below.

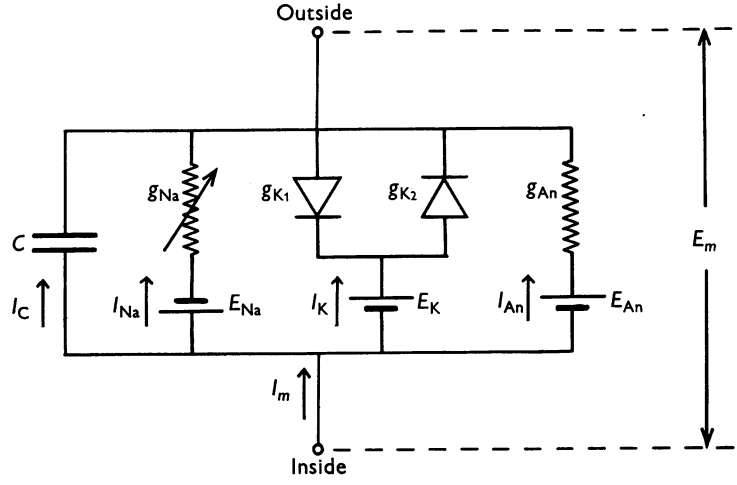

Fig. 1. Equivalent electrical circuit for Purkinje fibre membrane. Explanation in text.

The potassium current

The equations which will be used to describe the potassium current are based on Hutter & Noble's (1960) measurements of the current–voltage relations of Purkinje fibres in sodium-deficient solutions. In contrast to the situation in squid nerve, depolarization was found to *decrease* the membrane conductance (Hutter & Noble, 1960; Carmeliet, 1961). A small and slowly developed increase in conductance occurs when large depolarizing currents are used (Hutter & Noble, 1960) but this effect is not large enough for the conductance of the depolarized membrane to exceed the resting conductance.

The chloride conductance of normal resting cardiac muscle is very small (Carmeliet, 1961; Hutter & Noble, 1961) so that the fall in conductance on depolarization must be mainly, if not entirely, attributed to a fall in g_K. For the present purpose it will be assumed that all the current

measured in sodium-deficient solutions is carried by potassium. So far as the action potential mechanism is concerned this assumption will not matter greatly, since, over a large range of potentials, the potassium and chloride currents flow in the same direction. It does, however, mean that the potential dependent changes in g_K given by the equations described below are likely to be rather smaller than the true changes.

For the purpose of describing the potassium current mathematically, it is convenient to suppose that K ions may move through two types of channel in the membrane. In one the potassium conductance (g_{K_1}) is assumed to be an instantaneous function of the membrane potential and falls when the membrane is depolarized. In the other type of channel the conductance (g_{K_2}) slowly rises when the membrane is depolarized. These channels are represented in the circuit diagram (Fig. 1) by two parallel rectifiers, both of which are in series with the potassium battery. g_{K_1} is represented by a rectifier which passes inward current easily, while g_{K_2} is represented by a rectifier which passes outward current easily. A purely empirical equation will be used to describe g_{K_1}

$$g_{K_1} = 1{\cdot}2 \exp[(-E_m - 90)/50] + 0{\cdot}015 \exp[(E_m + 90)/60]. \quad (5)$$

Hutter & Noble's experiments do not provide any evidence for the assumption that g_K is an *instantaneous* function of E_m, because the discharging of the membrane capacity took so long (C_m is large and, when the membrane is depolarized, r_m is also large) that it was not possible to determine the changes occurring in g_K during the first 25–50 msec of the pulses, but it seemed to be the simplest assumption to make in the absence of information obtained under voltage-clamp conditions. It will be shown later, when the computed action potentials are compared with experimental records, that this assumption may well be wrong and that there may be a small delay in the changes in g_{K_1} following changes in E_m.

The conductance of the other type of channel (g_{K_2}) will be described by Hodgkin & Huxley's potassium current equations (Hodgkin & Huxley, 1952*d*, equations (6), (7), (12) and (13)), with two main modifications. First, the value of $\bar{g}_{K_2}$ (the maximum value of g_{K_2}) will be made much smaller than in nerve in order that the increase in g_{K_2} produced by depolarization should not offset the decrease in g_{K_1}. Secondly, the rate constants will be divided by 100 in order to take account of the very much slower onset of this effect in Purkinje fibres (Hutter & Noble, 1960). With these modifications the equations become

$$g_{K_2} = 1{\cdot}2n^4, \quad (6)$$

$$\frac{dn}{dt} = \alpha_n(1-n) - \beta_n n, \quad (7)$$

$$\alpha_n = \frac{0{\cdot}0001(-E_m - 50)}{\exp[(-E_m - 50)/10] - 1}, \quad (8)$$

$$\beta_n = 0{\cdot}002 \exp[(-E_m - 90)/80]. \quad (9)$$

The absolute values of the conductances have been adjusted to give a resting conductance (slope conductance at $E_m = -90$ mV) of about 1 mmho/cm^2 (Coraboeuf & Weidmann, 1954). The potassium equilibrium potential will be set at -100 mV so that the total potassium current is given by

$$I_K = (g_{K_1} + g_{K_2})(E_m + 100). \tag{10}$$

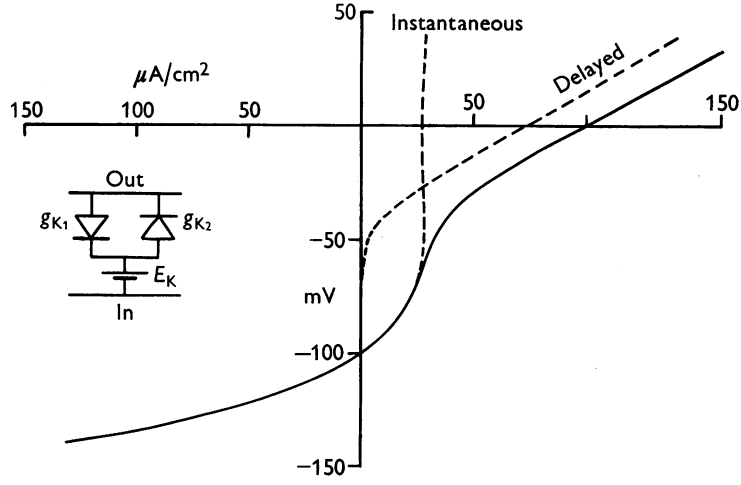

Fig. 2. Current–voltage relations described by K equations. Ordinate, membrane potential (mV); abscissa, K current in (μA/cm^2). Interrupted curves show current–voltage relations in the two types of K channel, as described in text. The continuous curve shows total steady-state current. The shape of this curve resembles that recorded experimentally, and over the voltage range of the action potential fits the curve obtained by Hutter & Noble (1960) reasonably closely when the experimental curve is corrected for the cable properties of the fibre, as described by Cole & Curtis (1941).

The current–voltage relations described by equations (5)–(10) are shown in Fig. 2. The interrupted curve labelled 'instantaneous' shows the current flowing in the first type of channel. The interrupted curve labelled 'delayed' shows the *steady-state* current flowing in the second type of channel, given by $g^{\infty}_{K_2}(E_m + 100)$, where $g^{\infty}_{K_2}$ is the value of g_{K_2} at a given potential after the potential has been held at this value for a long time. dn/dt is then zero and equations (6) and (7) give

$$g^{\infty}_{K_2} = 1{\cdot}2[\alpha_n/(\alpha_n + \beta_n)]^4. \tag{11}$$

The continuous curve shows the sum of the currents in the two channels. The constants in the equations have been chosen so that this curve should reproduce that recorded experimentally. Over the range of potentials covered by the action potential the shape of the curve is a reasonable fit with that recorded by Hutter & Noble (1960) after correction for the cable

properties of the fibre (the experimental curve was obtained by polarizing the membrane at one point with a micro-electrode and the correction for curves obtained in this way is given by Cole & Curtis (1941)). Outside this range the agreement is poor, especially when the membrane is hyperpolarized, when the potassium current is underestimated by the equations.

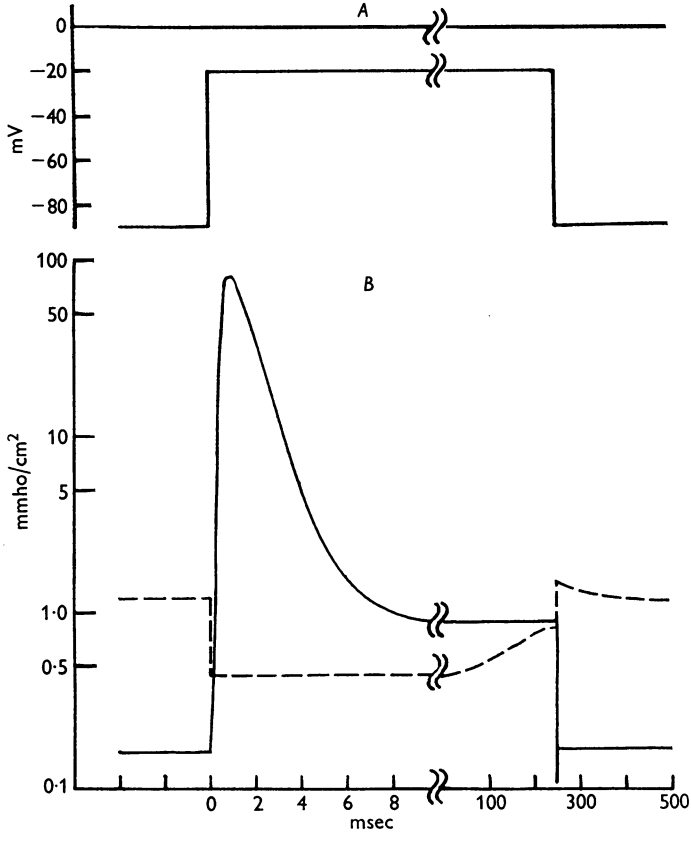

Fig. 3. Computed conductance changes occurring during depolarization of the 'membrane' from −90 to −20 mV. Ordinates: *A* membrane potential (mV); *B* ionic conductance (mmho/cm²) on a log. scale. Continuous curve, g_{Na}; interrupted curve, g_K. Abscissa: time (msec). Note change in time scale after 10 msec.

However, it did not seem worth while to try other values for the constants in the hope of obtaining a better fit because, in the computations described in this paper, the equations will not be used outside the voltage range of the action potential.

The time course of the changes in g_K given by these equations is shown in Fig. 3 (interrupted curve) in which the effect of a sudden change in E_m from

-90 mV to -20 mV is shown. g_K initially falls and then slowly rises during the period of depolarization (note the change in time scale after 10 msec). When the potential is suddenly returned to -90 mV, g_K rises above its resting value, towards which it then slowly falls. Some experimental evidence for this slow fall in g_K after depolarization has been obtained (Hutter & Noble, unpublished; Noble, 1961).

The sodium current

In squid nerve changes in the membrane potential have a dual effect on the sodium conductance (Hodgkin & Huxley, 1952*c*). When the membrane is suddenly depolarized there is initially a very large increase in g_{Na}, but, even if the depolarization is maintained, g_{Na} soon falls again to a low value. Moreover, the magnitude of the initial increase in g_{Na} depends on the previous value of the membrane potential. Hodgkin & Huxley described this behaviour by supposing that g_{Na} is determined by two variables, m and h, which vary with the membrane potential in opposite directions and with different time constants

$$g_{Na} = m^3 h \bar{g}_{Na}, \tag{12}$$

where $\bar{g}_{Na}$ is a constant and m and h obey the equations:

$$\frac{dm}{dt} = \alpha_m(1-m) - \beta_m m, \tag{13}$$

$$\frac{dh}{dt} = \alpha_h(1-h) - \beta_h h, \tag{14}$$

where α_m, β_m, α_h and β_h are functions of E_m.

The dependence of h on E_m describes the relation between the initial membrane potential and the maximum sodium current which may be produced by depolarization of the membrane. Using a modification of the voltage-clamp technique and using the maximum rate of depolarization as a measure of the sodium current, Weidmann (1955) showed that in Purkinje fibres this relation is very similar to that in squid nerve, except that the curve is shifted along the voltage axis by about 20 mV. His method did not allow accurate measurements of α_h and β_h but he did show that these are of the same order of magnitude and vary with E_m in the same way as in squid nerve. Thus the only modifications required in the equations for h is that the functions for α_h and β_h should be shifted along the voltage axis so as to make the relation between E_m and the steady-state value of h,

$$h_\infty = \alpha_h/(\alpha_h + \beta_h), \tag{15}$$

coincide with Weidmann's experimental curve. This was done by adjusting the constants determining the position of the curve until the

potential at which $h_\infty = 0{\cdot}5$ became about -71 mV (Weidmann, 1955). The equations for α_h and β_h obtained in this way are:

$$\alpha_h = 0{\cdot}17 \exp[(-E_m - 90)/20], \tag{16}$$

$$\beta_h = \left[\exp\left(\frac{-E_m - 42}{10}\right) + 1\right]^{-1}. \tag{17}$$

This procedure leaves the *shape* of the h_∞/E_m relation unaltered. In fact, Weidmann's curve for Purkinje fibres is slightly steeper than that for squid nerve, but, as he has pointed out, it is very likely that this is only due to differences in experimental technique.

In the voltage-clamp technique used by Weidmann, when the sodium conductance is greatly increased on depolarization of the membrane it is not possible to retain control of the membrane potential owing to the limitation on the amount of current which may be passed through a micro-electrode. He was therefore unable to obtain information on which to base equations for m. However, in view of the close similarity of the processes determining h in Purkinje fibres and in squid nerve, it seems reasonable to assume that the processes determining m are also similar. The choice of constants in the m equations must at present be a somewhat arbitrary procedure and the method used will be described in detail below (see Methods). The equations obtained are:

$$\alpha_m = \frac{0{\cdot}1(-E_m - 48)}{\exp[(-E_m - 48)/15] - 1}, \tag{18}$$

$$\beta_m = \frac{0{\cdot}12(E_m + 8)}{\exp[(E_m + 8)/5] - 1}. \tag{19}$$

In arriving at these equations it was assumed that a small component ($0{\cdot}14$ mmho/cm^2) of g_{Na} is independent of E_m and t. $\bar{g}_{Na}$ was set at 400 mmho/cm^2 and E_{Na} at 40 mV. When these values are inserted into equation (1) I_{Na} is given by

$$I_{Na} = (400m^3h + 0{\cdot}14)(E_m - 40). \tag{20}$$

The behaviour of these equations is of course very similar to that of Hodgkin & Huxley's (Hodgkin & Huxley, 1952*d*; Huxley, 1959*a*). It is, however, worth illustrating in order to note the changes which occur when a *long-lasting* depolarization is applied. This is shown in Fig. 3 (continuous curve). When E_m is suddenly changed from -90 to -20 mV it can be seen that, following the large transient increase in g_{Na}, there is a small maintained increase which persists throughout the period of the depolarization. The steady-state Na current therefore increases in spite of the decrease in the Na electrochemical potential gradient. This property allows the

equations to be extended to describe long-lasting action potentials without any serious modification to the sodium current equations (cf. Fitzhugh, 1960).

METHODS

Method of obtaining equations for α_m and β_m

In the absence of any direct experimental evidence on which to base equations for m in cardiac muscle it is not possible to describe the sodium current fully without using the action potential itself as a source of information. The problem then becomes: given the shape of the action potential and equations for h and for I_K, what equations are required to describe m? A number of different equations for α_m and β_m were tried in order to see whether functions of the same general form as Hodgkin & Huxley's could be used. This turned out to be the

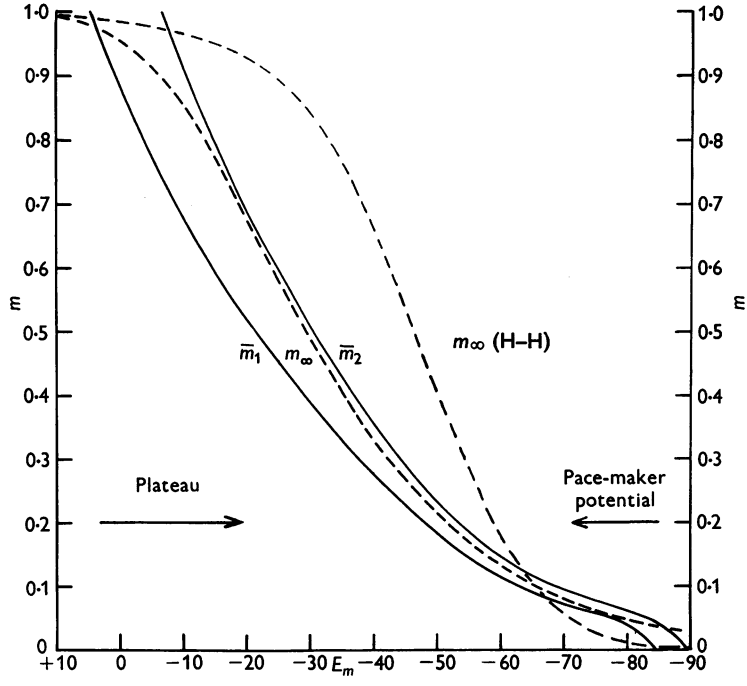

Fig. 4. Relations between m (ordinate) and membrane potential (abscissa). $\bar{m}_1$ is given by equation (22); $\bar{m}_2$ by equation (23); m_∞ by equations (18), (19) and (21); m_∞ (H–H) by equations (21), (24) and (25). Explanation in text.

case and it proved relatively easy to obtain solutions which resemble the Purkinje fibre action potential. However, it proved much more difficult to find equations for m which would also allow pace-maker activity to occur. The method of obtaining the constants by simple trial and error is excessively tedious and would have proved very costly in terms of computer time, so that it became essential to find a more direct method.

The way in which equations (18) and (19) were obtained is illustrated by Fig. 4, in which m is plotted against E_m. It was convenient to take $\bar{g}_{Na}$ as 400 mmho/cm^2 and to assume that 0·14 mmho/cm^2 is independent of E_m and t. This does not necessarily mean that g_{Na} in some channels is in fact independent of E_m and t in cardiac muscle, but it made a little easier the

process of finding functions for α_m and β_m which allow pace-maker activity to occur. The continuous curve labelled $\overline{m}_1$ in Fig. 4 shows the value which m_∞, given by

$$m_\infty = \alpha_m/(\alpha_m+\beta_m), \tag{21}$$

must have at each potential in order that the steady-state sodium current should be equal and opposite to the potassium current when $n = 0$. This is given by

$$\overline{m}_1 = \left(\frac{[g_{K_1}(E_m+100)/(40-E_m)]-0{\cdot}14}{400h_\infty}\right)^{\frac{1}{3}}, \tag{22}$$

and is applicable at the end of diastole and during the spike of the action potential when n is small enough for g_{K_2} to be neglected. The continuous curve labelled $\overline{m}_2$ shows the same relation when n has the value which it would have if E_m were held constant for a long time at a potential corresponding to the termination of the plateau. $E_m = -30$ mV was chosen and n_∞ is then very nearly 0·72. $\overline{m}_2$ is given by

$$\overline{m}_2 = \left(\frac{[(g_{K_1}+1{\cdot}2n^4)(E_m+100)/(40-E_m)]-0{\cdot}14}{400\,h_\infty}\right)^{\frac{1}{3}}. \tag{23}$$

Now in order to obtain solutions describing both action and pace-maker potentials the functions for α_m and β_m must satisfy two requirements:

(1) $m_\infty < \overline{m}_2$ for all values of E_m positive to the maximum diastolic potential (E_m approximately -90 mV), since for repolarization to occur the sodium current must be less than the potassium current.

(2) $m_\infty > \overline{m}_1$ for all values of E_m negative to the potential at the beginning of the plateau. If, for example, $m_\infty = \overline{m}_1$ at some potential around -90 mV then this potential would form a resting potential and pace-maker activity would not occur.

The curve labelled m_∞ in Fig. 4 satisfies these conditions and is given by equations (18), (19) and (21). The individual functions for α_m and β_m are plotted in Fig. 5 for comparison with those of Hodgkin & Huxley, which after adjustment along the voltage axis by the same amount as the h equations (see above) become

$$\alpha_m = \frac{0{\cdot}1(-E_m-47)}{\exp[(-E_m-47)/10]-1}. \tag{24}$$

$$\beta_m = 4\exp[(-E_m-72)/18]. \tag{25}$$

These equations are plotted as interrupted curves in Fig. 5 and the m_∞/E_m relation is plotted as an interrupted curve labelled m_∞ (H–H) in Fig. 4. So far as the *shape* of the curves is concerned, the main difference between my equations and those of Hodgkin & Huxley is that m_∞ and β_m vary less steeply with E_m. Thus the values $m_\infty = 0{\cdot}5$ and $m = 0{\cdot}1$ are separated by about 35 mV in my equations and by only about 20 mV in Hodgkin & Huxley's equations. These differences will be discussed in greater detail later (see Discussion).

When it was desired to obtain solutions not showing pace-maker activity g_K was increased by 0·1 mmho/cm^2, when condition (2) above is no longer satisfied.

Numerical computation

The integration of the four simultaneous differential equations (4), (7), (13) and (14) was done on the London University digital computer 'Mercury', using a numerical approximation (the Runge–Kutta rule). Solutions for the rapid changes occurring during the spike of the action potential were obtained by using a step length of integration, Δt, of 0·1 msec. It was found that integration at shorter step lengths did not produce an appreciably different result.

By comparison with the initial spike, the plateau and pace-maker potential are very long-lasting indeed and to obtain solutions for these parts of the action potential with $\Delta t = 0{\cdot}1$ msec more than 60 min of computer time was required. This could not be reduced simply by increasing Δt, because computations involving differential equations with very small time

constants become unstable when $\Delta t > 2{\cdot}8\, T_{\text{min.}}$, where $T_{\text{min.}}$ is the smallest time constant in the system (Carr, 1958; N.P.L., 1961). This difficulty was overcome by making m an explicit function of only E_m during the plateau and pace-maker potential. This is justified, since the time constants for m are small enough compared to the duration of these phases of the action potential to allow the assumption that, at each value of E_m, m has its steady-state value, m_∞. Equation (21) may then be used to compute m. The problem now reduces to the integra-

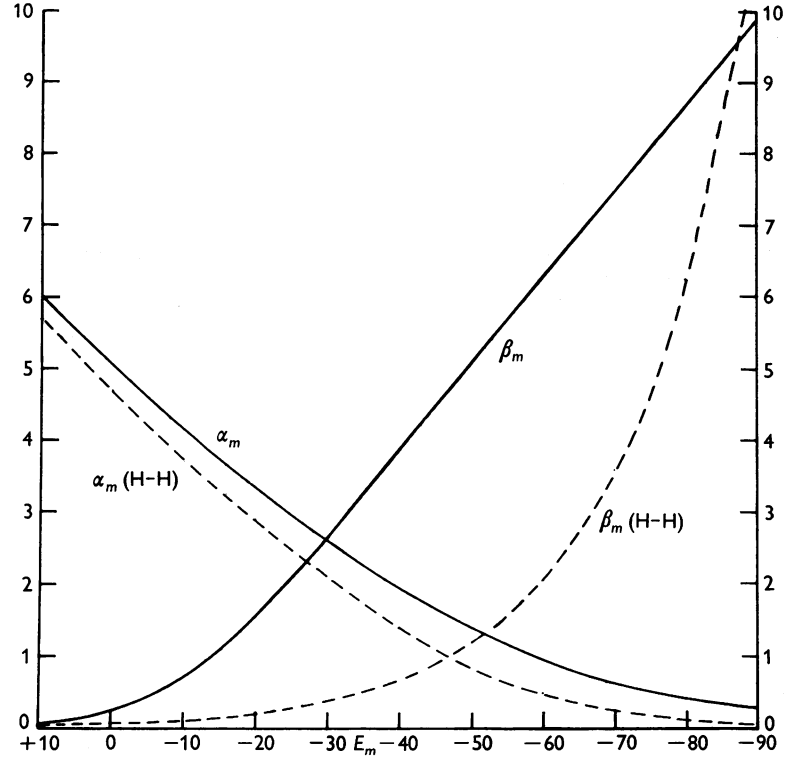

Fig. 5. Comparison of modified functions for α_m and β_m with those of Hodgkin & Huxley. Continuous curves: modified functions given by equations (18) and (19). Interrupted curves: Hodgkin & Huxley's m functions after adjustment along voltage axis by same amount as for h equations. These curves are given by equations (24) and (25). Note that β_m changes less rapidly with E_m in modified function than in original Hodgkin–Huxley function.

tion of three simultaneous equations and, since the time constants for h are about 10 times larger than those for m, Δt can be increased to 1 msec without introducing appreciable error. This was checked by comparing results obtained at $\Delta t = 0{\cdot}1$ msec with equation (13) to compute m with those obtained at $\Delta t = 1$ msec with equation (21). The computer programme was arranged so that equation (21) was used when $dE_m/dt < 0{\cdot}5$ V/sec.

In order to start the computation, the initial values of E_m, m, h and n have to be given. These were obtained by choosing an initial potential at about the middle of the pace-maker potential, when dE_m/dt is very small. m and h could therefore be given their steady-state values (m_∞ and h_∞) without introducing appreciable error. A guess was then made for the

initial value of n. A small error here is not critical, however, and after one cycle the initial value chosen for n has no influence on the solution, apart from determining its position on the time scale.

Results were printed out by the machine usually after every 10 integration steps. In addition to E_m and t, the following were printed out when required: m, h, n, g_{Na}, g_K, Na efflux, Na influx, K efflux, K influx, net Na gain, net K loss. Where appropriate these are plotted in the illustrations in addition to the potential changes. Curves relating to Na are continuous, whereas curves relating to K are interrupted.

RESULTS

Computed potentials and conductances

The solution to the equations was computed over two cycles and is shown in Fig. 6. It can be seen that the shape of the potential wave (curve *A*) closely resembles that recorded experimentally in Purkinje fibres and shows the characteristic spike, followed by a plateau lasting

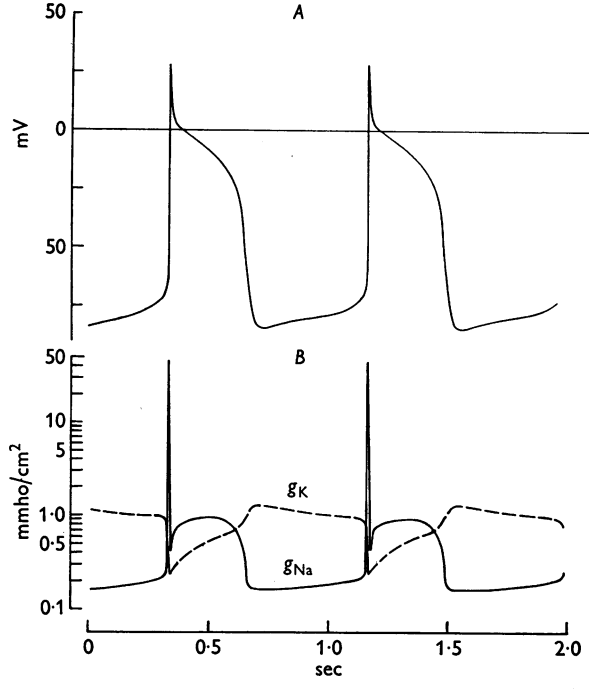

Fig. 6. *A*, computed action and pace-maker potentials. *B*, time course of conductance changes on a log. scale. Continuous curve, g_{Na}: interrupted curve, g_K.

about 300 msec which is terminated by a faster phase of repolarization. The membrane then slowly depolarizes again—the pace-maker potential—until the threshold is reached and another action potential is initiated.

Only in one major respect does the computed action potential fail to

reproduce that recorded experimentally. The maximum rate of depolarization, $dE_m/dt_{max.}$, during the spike of the computed action potential is about 100 V/sec. This is very much less than that recorded experimentally: action potentials initiated from about -70 mV (as in the computed action potential in Fig. 6) show a maximum rate of depolarization of about 300 V/sec (Weidmann, 1955). The relation between E_m and $dE_m/dt_{max.}$ is very steep at about $-$ 70 mV (Weidmann, 1955) and a better comparison may be obtained by initiating the action potentials from a potential at

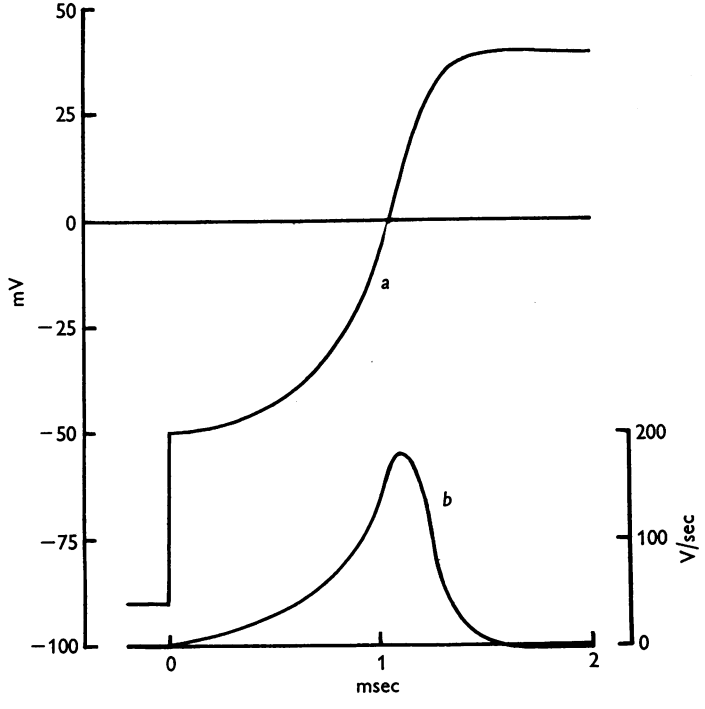

Fig. 7. *a*, Early part of computed action potential initiated by suddenly displacing E_m from -90 to -50 mV. *b*, Rate of change of membrane potential, dE_m/dt, (V/sec).

which h is very nearly 1, so that all the sodium carriers (or sites) are readily available for sodium transport. In these circumstances the value for $dE_m/dt_{max.}$ obtained experimentally is about 800 V/sec (Draper & Weidmann, 1951; Weidmann, 1956*b*). When the computed action potential is initiated from -90 mV, $dE_m/dt_{max.}$ is only 180 V/sec (Fig. 7). The possible reasons for this discrepancy will be discussed later.

The time course of the computed conductance changes is shown in Fig. 6*B*. A logarithmic scale was chosen in order to accommodate the large changes which occur in g_{Na}. During the spike of the action potential g_{Na}

rises to a very high value because m rises much faster than h falls. Within a few milliseconds the fall in h reduces g_{Na} again; the inactivation is not complete, however, and, after an 'undershoot', g_{Na} settles down to a fairly constant plateau value which is about 8 times larger than the lowest value reached in diastole. The relative constancy of g_{Na} in spite of changes in E_m during the plateau is due to the fact that, over this range of potentials, m and h change in opposite directions in such a way that m^3h remains almost constant. At the end of the plateau, during the final rapid phase of repolarization, the rise in h no longer fully counteracts the fall in m, and g_{Na} then falls to its diastolic value.

By contrast, g_K *falls* at the beginning of the action potential as a result of the fall in g_{K_1}. During the plateau g_{K_2} slowly rises, but the total g_K remains below the end-diastolic value throughout the duration of the plateau. A further increase in g_K occurs at the end of the action potential when g_{K_1} increases as a result of the repolarization of the membrane. g_{K_2} takes some time to fall again, so that g_K exceeds its end-diastolic value for several hundred milliseconds during the pace-maker potential.

The *total* membrane conductance, $g_{Na}+g_K$, increases about 50 times during the spike of the action potential in Fig. 6*A* and almost 100 times during the faster spike shown in Fig. 7. This is in good agreement with the experimental observation of Weidmann (1951), who found the ratio of resting membrane conductance to maximum active conductance to be about 1:100. During the plateau the total conductance is much smaller and, at the beginning of the plateau, is about the same as the end-diastolic conductance. Since g_{Na} remains fairly constant while g_K increases, the total conductance rises during the plateau. However, this does not conflict with Weidmann's observation that the membrane impedance increases during the plateau (see Impedance changes, p. 337).

Computed currents and fluxes

The changes in g_{Na} and g_K which occur during the action potential to some extent resemble those produced by an applied 'square-wave' voltage change of similar magnitude to the plateau (Fig. 3) although, in the case of the action potential, the voltage changes themselves are in turn produced by the conductance changes. During an applied 'square-wave' voltage change current would have to be supplied to the membrane to keep the potential constant, and this is the current which would be recorded by a 'voltage-clamp' technique. The action potential, on the other hand, requires no externally applied current, all the current being supplied by the fibre itself, and in the case of a 'membrane' action potential the relation between ionic current and the potential changes is a fairly simple one, dE_m/dt being proportional to the net ionic current.

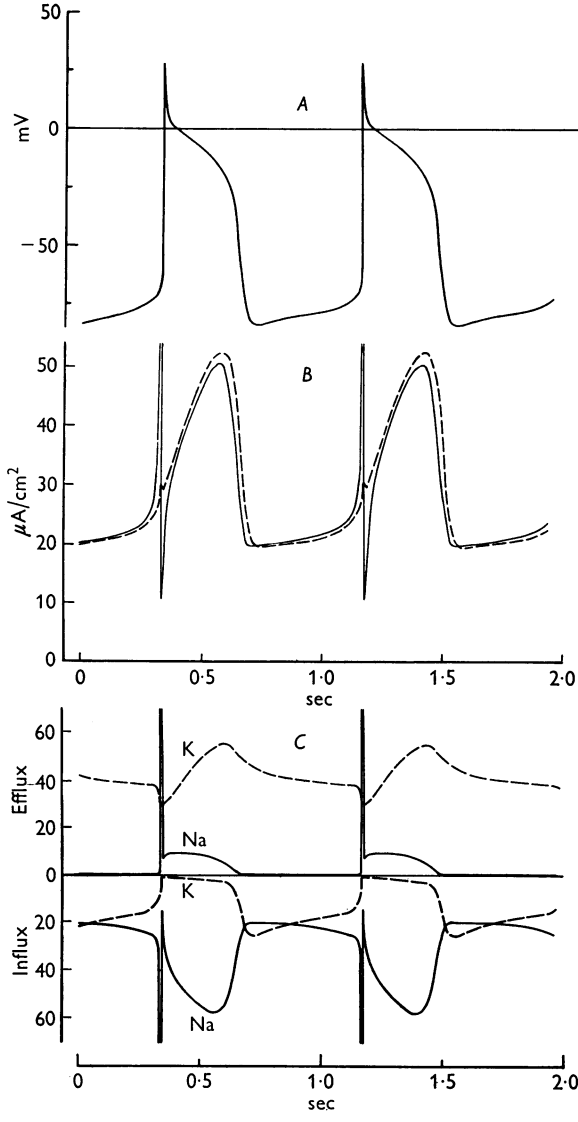

Fig. 8. *A*, computed action and pace-maker potentials (as in Fig. 6*A*). *B*, computed ionic currents. Continuous curve, I_{Na}; interrupted curve, I_K. The peak Na current was about 1200 μA/cm^2 and is not shown on the scale used. dE_m/dt is positive when $I_{Na} > I_K$ and is negative when $I_{Na} < I_K$. *C*, Ionic fluxes given by equations (26) and (27). Effluxes are plotted upwards above the abscissa; influxes are plotted downwards below the abscissa.

The computed Na and K currents flowing during the action potential are shown in Fig. 8*B*. Although the ionic currents flow in opposite directions (Na inwards, K outwards) they are plotted here in the same direction. This makes it easier to observe changes in the net ionic current ($I_{Na}+I_K$), which is then simply the difference between the two curves.

During the rising phase of the action potential spike I_{Na} (continuous curve) greatly exceeds I_K (interrupted curve). The peak Na current is not shown in the diagram, as it rose to just over 1200μA/cm^2. It is this intense inward Na current which produces the rapid depolarization. During the falling phase of the spike I_{Na} falls to its lowest value ($\simeq$ 10 μA/cm^2), partly as a result of the decrease in the Na electrochemical potential gradient and partly as a result of the low value to which g_{Na} falls at this stage (Fig. 6*B*). Since I_K is continuously rising (in spite of the fall in g_K), it now exceeds I_{Na} by almost 20 μA/cm^2, so that the potential falls fairly rapidly towards its value at the beginning of the plateau. Throughout the plateau I_K is only slightly greater than I_{Na}, so that the membrane repolarizes very slowly. This difference increases towards the end of the plateau and the membrane then repolarizes more rapidly. Both currents now decrease: I_{Na} falls because the decrease in g_{Na} (Fig. 6*B*) offsets the increase in the Na electrochemical potential gradient, while I_K falls because the decrease in the K electrochemical potential gradient offsets the increase in g_K (Fig. 6*B*). I_{Na} now slightly exceeds I_K and the membrane slowly depolarizes again.

The average magnitudes of the Na and K currents during the pacemaker potential are just over 20 μA/cm^2, whereas during the action potential the average currents are about 40 μA/cm^2. Thus the action potential involves a twofold increase in the rate at which the fibre gains Na and loses K. This increase is, however, much less than it would be if g_K were not to fall on depolarization of the membrane. In terms of chemical quantities, the K loss or Na gain during one action potential amounts to 161 pmole/cm^2. Since the resting loss or gain during a similar period is 83 pmole/cm^2, the extra K loss or Na gain during one action potential is 77 pmole/cm^2. Of this, only about 13·5 pmole is used in changing the charge on the membrane capacity, the remaining 63·5 pmole being 'wasted' as the result of the increased Na and K currents overlapping each other over a considerable period of time (Fig. 8*B*). This 'wastage' forms a larger fraction of the ionic movements than in squid nerve (Hodgkin & Huxley, 1952*d*) and represents the 'cost' to the fibre of maintaining the plateau of the action potential.

The efflux and influx components of the ionic currents were computed on the assumption that the independence principle applies to Purkinje fibres. This principle states that the influx and efflux of a given ion species are independent of one another, i.e. the influx is independent of the intra-

cellular concentration, while the efflux is independent of the extracellular concentration. This assumption leads to the following equations for the effluxes (Hodgkin & Huxley, 1952*d*):

$$\text{Na efflux} = I_{\text{Na}}/[\exp((E_{\text{Na}} - E_m)F/RT) - 1], \quad (26)$$

$$\text{K efflux} = I_{\text{K}}/[\exp((E_{\text{K}} - E_m)F/RT) - 1]. \quad (27)$$

The influxes are then given by the differences between the currents and the effluxes. Hodgkin & Huxley showed that the independence principle holds very well in the case of Na movement in squid nerve, but no experimental confirmation of the principle yet exists in the case of cardiac muscle. The application of these equations to Purkinje fibres therefore requires caution and the presence of any appreciable degree of interaction during the movement of ions through the membrane would invalidate them.

In Fig. 8*C* the effluxes are plotted above the abscissa (continuous curve, Na; interrupted curve, K) while the influxes are plotted below the abscissa. The most surprising feature is the very small increase in K efflux which occurs during the action potential. When averaged out over the duration of one cycle, this increase amounts to only about 10% of the diastolic efflux. This is in striking contrast to the large increase in K efflux during the squid-nerve action potential observed by Keynes (1951) and computed by Hodgkin & Huxley (1952*d*). In Purkinje fibres most of the increase in the computed K current results from a very large fall in K influx. In the case of sodium both influx and efflux increase during the action potential. The peak Na fluxes are not shown in the illustration. The peak influx was nearly 1500 μA/cm^2 and the peak efflux was nearly 300 μA/cm^2.

The correlation of these computed fluxes with the experimental information at present available in cardiac muscle will be discussed later (see Discussion).

Current–voltage relations

A simpler, though more approximate, description of the mechanism of the action and pace-maker potentials may be obtained by plotting Na and K current–voltage relations at different times during the cycle (cf. Hodgkin, Huxley & Katz, 1949). This has been done in Fig. 9. The ordinate is the membrane potential (mV) and the abscissa is the ionic current (μA/cm^2). Although the Na and K currents flow in opposite directions, they have been plotted here in the same direction so that intersections between the curves represent points at which the currents are equal and opposite. The interrupted curves show the *instantaneous* K current–voltage relations given by equations (5), (6) and (10) with n having values appropriate to the beginning of the action potential (0 msec, $n = 0{\cdot}32$), two stages during the plateau (100 msec, $n = 0{\cdot}58$; 200 msec, $n = 0{\cdot}68$) and at the end of

the plateau (280 msec, $n = 0{\cdot}72$). These curves also apply at points during the pace-maker potential, but the temporal order is then reversed as n is then falling instead of rising. The continuous curves are Na current–voltage relations. The line intersecting the 0 msec K curve at the point A is the *instantaneous* Na current–voltage relation at the peak of the action potential

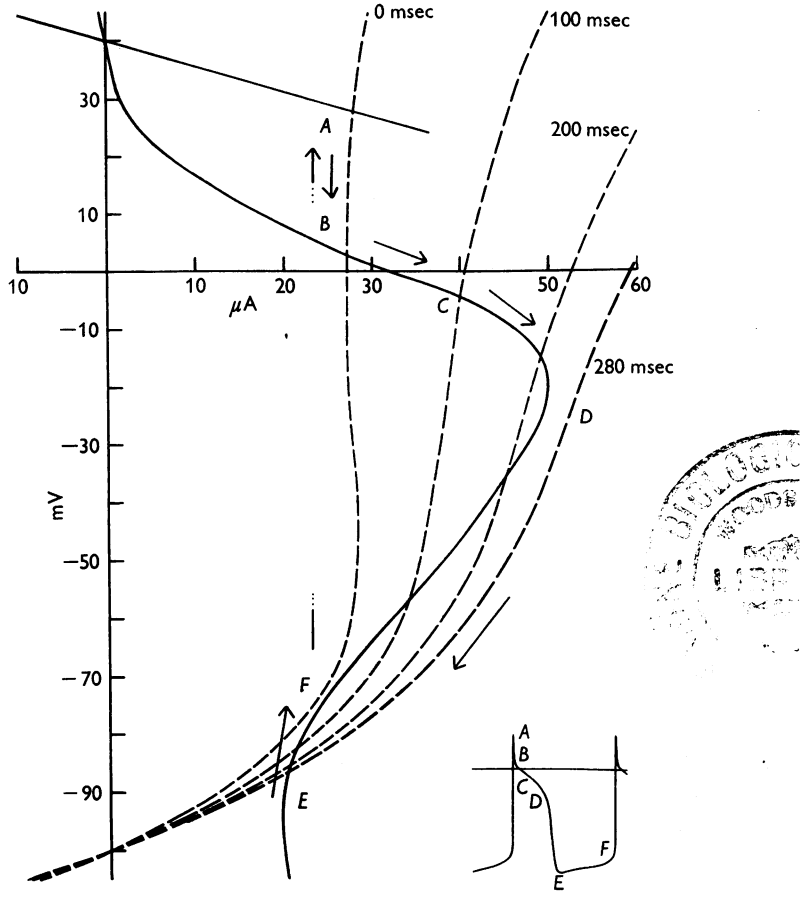

Fig. 9. Ionic current–voltage relations. Ordinate, membrane potential (mV); abscissa, ionic current (μA/cm^2). Interrupted curves are instantaneous K current–voltage relations at various stages during the action potential. The continuous curves are Na current–voltage relations. Points A–F correspond to the stages indicated on the computed action potential shown in inset. Explanation in text.

spike. This is given by equations (12) and (20) with $m = 0{\cdot}9996$ and $h = 0{\cdot}010$. The other continuous curve shows the *steady-state* Na current–voltage relation given by equations (12), (15), (20) and (21). Since changes in m and h follow changes in E_m fairly closely during the slower phases of

the action potential, this curve gives an approximate estimate of the Na current at different voltages during the plateau and pace-maker potential.

When dE_m/dt is small the net ionic current must be small, so that the Na and K currents are nearly equal and opposite (see Fig. 8). Some of the intersections in Fig. 9 therefore closely correspond to the values of the potentials and currents occurring at various instants during the action potential. The points labelled A–F correspond to the stages during the cycle indicated in the inset. Point A corresponds to the peak of the action potential spike, when g_{Na} is very large. As the Na-carrying system becomes inactivated g_{Na} approaches its steady-state value at the beginning of the plateau, and the potential falls to point B. I_K then increases, so that the potential slowly falls, passing through point C, until the K curve no longer intersects the Na steady-state curve in the region of the plateau (point D). The K current now exceeds the steady-state Na current at all potentials above the point E, so that the plateau can no longer be maintained and the rapid phase of repolarization commences. During this phase the steady-state Na curve does not give a good approximation to the sodium current, because the potential changes too rapidly for h to approximate closely enough to its steady-state value at each potential. Thus, at a membrane potential of -50 mV the Na current during repolarization is 27 μA/cm^2 (Fig. 8B), whereas the steady-state current is about 38 μA/cm^2 (Fig. 9). When the point of maximum repolarization, E, is reached the Na and K curves once again intersect. The K current–voltage curve now 'swings' back again towards the 0 msec curve and the potential slowly rises until the point F is reached at the end of the pace-maker potential. The Na and K curves now no longer intersect in the pace-maker region, the membrane depolarizes more rapidly and another action potential is initiated. During this phase the Na current is very much greater than the steady-state current, and the potential rapidly changes to point A. The cycle then repeats itself.

The mechanism of the pace-maker potential is thus very similar to that of the plateau. Both can be approximately represented as a point of intersection moving along the steady-state Na current–voltage curve.

In these equations there is one potential at which the steady-state Na curve intersects the *steady-state* K curve. The latter is the continuous curve in Fig. 2, but is not shown in Fig. 9. Its point of intersection with the Na curve occurs at about -32 mV and a constant potential at this point therefore corresponds to a second solution to the equations. However, this solution is unstable because it occurs at a potential at which the total membrane slope conductance is negative. A deflexion, however small, in the repolarizing direction would reduce I_{Na} more than I_K, so that the repolarization would become regenerative. Similarly, a deflexion in the depolarizing direction would increase I_{Na} more than I_K, which would lead to a regenerative depolarization.

Only small modifications to the equations are required to make such a point occur outside the region of negative slope conductance. If g_K were increased by about 0·1 mmho/cm², a point of intersection would occur in the region of the pace-maker potential. The potential would then fail to reach the point F spontaneously and the system would correspond to a normal quiescent fibre. On the other hand, if $\bar{g}_{K_2}$ were reduced by about 35 % a 'stable state' would occur in the region of the plateau at about −20 mV. This would correspond to a fibre which becomes temporarily or permanently arrested on the plateau, as is in fact observed when Purkinje fibres are cooled sufficiently (Trautwein, Gottstein & Federschmidt, 1953; Coraboeuf & Weidmann, 1954; Chang & Schmidt, 1960).

Impedance changes

It has been shown above that the increase in membrane conductance during the spike of the computed action potential agrees well with that observed experimentally by Weidmann (1951). Weidmann also recorded the changes in impedance occurring during the slower phases of the Purkinje fibre action potential. Although he used square-wave current pulses and has expressed his results in terms of membrane 'resistance' (Weidmann, 1956*b*, Fig. 16) it is clear from his record that, at least during the plateau, the electrotonic potentials did not reach completion, so that his experiment measured a quantity which depended on the membrane reactance as well as the membrane resistance. An equation for sinusoidal current was therefore employed in order to reproduce Weidmann's result on the computed response. The currents used in obtaining the curves shown in Fig. 10 are

$$I_m = 7 \sin\left[\frac{2\pi}{50}(t+b)\right] \mu\text{A/cm}^2 \qquad (29)$$

with $b = 0, 15, 30$. This gives three currents of the same period (50 msec) but with different phase shifts (b). The integrations were started at the peak of an unmodulated action potential and the resulting potential curves have been superimposed in Fig. 10. So far as the main features are concerned the agreement between this and Weidmann's experimental record is very good. The impedance rises during the plateau, falls again at the end of repolarization and then rises slightly during the pace-maker potential. The rise in impedance during the plateau may appear surprising in view of the fact that the total membrane conductance ($g_{Na}+g_K$) increases during this time (Fig. 6*B*). The reason for this is that m, h, n and g_{K_1} vary periodically as a result of the periodic changes in E_m, so that g_K and more particularly g_{Na} have values which depend on the phase of the applied current. The factors determining the amplitude of the voltage wave are not therefore the ionic chord conductances (g_K, g_{Na}) but the ionic *slope* conductances (dI_K/dE_m, dI_{Na}/dE_m). If the period of the alternating current is long compared with the Na time constants, but short compared with the K time constants, the slope conductances will be approximately equal to the

reciprocal slopes of the curves shown in Fig. 9; from which it can be seen that the Na slope conductance falls during the plateau and eventually becomes negative at about -20 mV. Although the K slope conductance rises, it does not do so sufficiently to prevent the total slope conductance from falling. The membrane impedance therefore rises during the plateau. This is a rather striking illustration of the fact that changes in membrane impedance do not necessarily closely reflect changes in ionic conductance and, as in this case, may even appear to indicate changes in the opposite direction to those which are actually occurring.

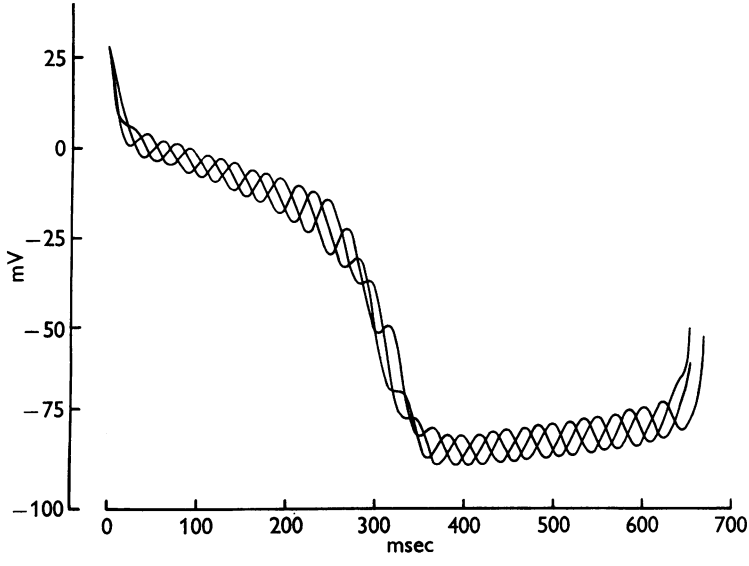

Fig. 10. Variation in membrane impedance during action and pace-maker potentials. Three superimposed potential curves obtained by setting I_m equal to sinusoidal currents given by equation (29). The impedance rises during the plateau, falls at the end of repolarization and then rises slightly during the pace-maker potential.

The rise in impedance during the pace-maker potential is due to three factors: the slow fall in g_{K_2}, the fall in g_{K_1} consequent upon depolarization and the increasing negativity of the Na slope conductance (see Fig. 9).

Vector analysis of the impedance changes in Fig. 10 into parallel resistive and reactive components gave a rather complicated result. In particular, the parallel reactance does not remain constant, as it depends not only on the constant membrane capacity assumed in the equations but also on a variable 'anomalous' reactance attributable to the periodic changes in g_{Na} and g_K described above.

Regenerative repolarization

When a large enough repolarizing current is passed through the membrane during the plateau of the action potential, an all-or-nothing repolarization is initiated (Weidmann, 1951, 1956*b*). That this type of behaviour may be reproduced by the Hodgkin–Huxley equations, and modifications of them, is now well known (Huxley, 1959*a*, *b*; Fitzhugh, 1960; George & Johnson, 1961). The behaviour of the equations used here is illustrated in Fig. 11, which shows the potential changes produced by adding square-wave current pulses at two different times during the

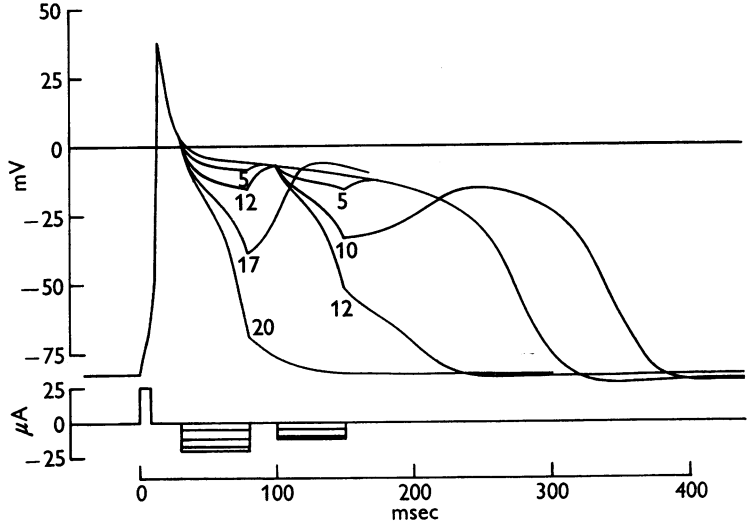

Fig. 11. Effect of current pulses on the computed membrane potential during the plateau. Current strengths are indicated by current plot at bottom of illustration and by the figures (in μA/cm^2) on the potential curves. Description in text.

plateau. When currents above a certain threshold strength are added, the potential does not return to the plateau when the current pulse is terminated. Instead, the potential returns to the resting potential. The threshold for this phenomenon is larger at the beginning of the plateau than at the end (cf. Fitzhugh, 1960) and, during the early part of the plateau, is about 40–50 mV negative to the plateau potential. This is less negative than the threshold observed by Weidmann when recording the potential changes very close to a polarizing electrode (Weidmann, 1956*b*, Fig. 25*B*) but is greater than that observed when the electrodes are inserted one or two space constants apart (Weidmann, 1956*b*, Fig. 25*C*). A difference of this kind is to be expected, since, in the first case when the applied current is switched off local circuit currents will flow in such a direction as to bring

the potential back to the plateau, so that the threshold voltage displacement will be greater than in the case where the membrane is polarized uniformly, as it is in the case of the computed action potentials. When the potential is recorded at some distance away from the polarizing electrode, the converse will apply and the local circuit current will flow through the membrane in the opposite direction. A further complication arises here because the regenerative repolarization response is probably propagated (Weidmann, 1951). This effect is not of course reproduced in computed 'membrane' action potentials.

A current which just fails to initiate repolarization (e.g. 10 μA in the middle of the plateau) *prolongs* the action potential. This effect results from the dependence of the rate constants of the 'delayed' potassium channels, α_n and β_n, on E_m so that g_{K_2} rises more slowly when the potential is altered by the repolarizing current than it does during the normal action potential. When the current is terminated, and the potential returns to the plateau, more time is required for g_{K_2} to reach the value required to bring about repolarization. Such a prolongation has been observed in Purkinje fibres (Weidmann, 1956*b*, Fig. 26) but the effect is not as large as in the computed action potential. Again, this difference may be due to the difference in the way in which the current is applied. In the experimentally recorded action potentials the current was not applied uniformly, so that local circuit currents occurred which are absent in the computed response.

These differences between the computed and experimentally recorded action potentials in their responses to applied currents are minor ones but are difficult to deal with satisfactorily in qualitative terms. It is clearly desirable that solutions for propagated action potentials with locally applied currents should be computed to test these points.

Repetitive stimulation

Another property of cardiac muscle which may be accounted for by these equations is the shortening of the duration of the action potential produced by an increase in the frequency of stimulation (Carmeliet, 1955*a*, *b*; Hoffmann & Suckling, 1954; Trautwein & Dudel, 1954). This results from the slow time course of the decay of g_{K_2} after the end of the action potential. If two action potentials are initiated in rapid succession, the second is shorter than the first because g_{K_2} starts at a higher value and so takes less time to rise to the value required to initiate repolarization of the membrane. A potassium current system with long time constants is also a feature of Fitzhugh's (1960) modification of the Hodgkin–Huxley equations and he has already shown how this accounts for the frequency–duration relation.

An interesting consequence of this relation is that an alternation in the duration of successive action potentials is observed when a resting fibre is suddenly stimulated at a high enough frequency. This effect is shown on the computed action potential in Fig. 12. The interrupted curve shows the changes which occur in n (the variable determining g_{K_2}). In the 'resting fibre' n is small, g_{K_2} is virtually zero, so that during the *first* action potential n takes a long time to rise to the value required to initiate repolarization. The *second* action potential follows very soon after the first, while n is still fairly large. Much less time is therefore required for n to rise again, so that the second action potential is very much shorter than the first. This degree of shortening represents nearly the maximum obtainable from an increase

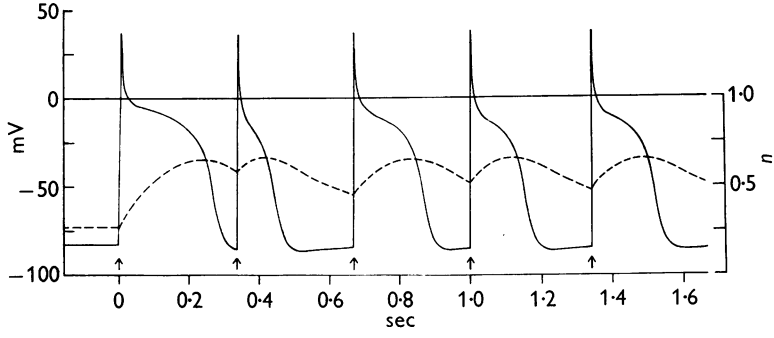

Fig. 12. Effect of repetitive stimulation on the computed action potential (continuous curve). Interrupted curve shows the changes which occur in n. 'Fibre' made 'quiescent' by adding 0·1 mmho/cm² to g_K and then suddenly stimulated at a frequency of 3/sec. Note alternation in duration of action potentials.

in frequency and is similar to that observed by Trautwein & Dudel (1954), who recorded action potentials down to durations of about 20% of the low-frequency duration. The *third* action potential follows after a longer 'diastole' than that which preceded the second, so that it is longer than the second although shorter than the first. An alternation of this kind persists for several action potentials before the duration finally reaches a stable value. This type of behaviour is often observed in cardiac muscle during sudden increases in frequency or on stimulation of a previously quiescent fibre (e.g. Hoffmann & Suckling, 1954; Schütz, 1936).

There is, however, one feature of the effect of frequency on duration which is not accounted for by these equations. After a period of high-frequency stimulation the action potential duration may take some time to return completely to normal, even though the fibre is stimulated at a constant low frequency (e.g. Carmeliet, 1955*a*, *b*; Hoffmann & Cranefield, 1960, Fig. 7–2). It seems therefore that some other factor must be involved

in addition to the one described here. This may be the time required for the restoration of ionic concentration gradients after a period of activity, as suggested by Carmeliet (1955*b*).

The influence of permeability changes

The changes in duration produced by alterations in the frequency of stimulation mainly involve changes in the duration of the plateau, the other phases of the action potential being relatively unaffected. The same also applies when the action potential duration is altered by changes in the ionic permeabilities or in the ionic environment. In spontaneously beating fibres the frequency is also very sensitive to permeability changes.

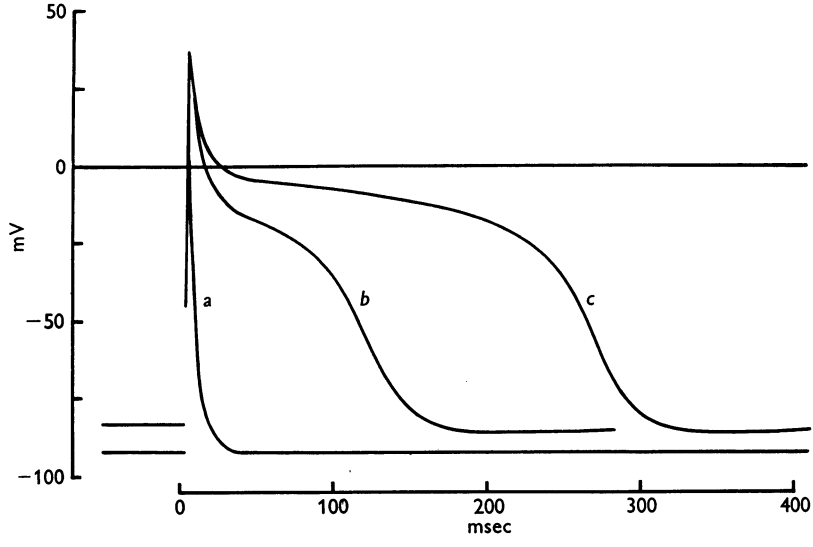

Fig. 13. Effect of additional ionic conductances on the duration of the computed action potential. *a*, No additional conductance. *b*, Additional conductance of 0·2 mmho/cm² with equilibrium potential at the resting potential. *c*, Effect of increasing g_K by 1·0 mmho/cm².

Figure 13 shows the effect of additional conductances on the shape of the computed action potential. The addition of a conductance of 0·2 mmho/cm² with an equilibrium potential at the resting potential approximately halves the duration of the plateau (curve *b*), which is similar to the effect produced by substituting Cl by NO_3 ions on the action potentials of Purkinje and ventricular fibres (Carmeliet, 1961; Hutter & Noble, 1961). An additional g_K of 1·0 mmho/cm² has a very striking effect which is shown in curve *c*. The plateau is now completely absent and the action potential becomes very short indeed. This resembles the effect produced on the sinus

venosus action potential when g_K is increased by stimulation of the vagus nerve (Hutter & Trautwein, 1956). The conductance increase assumed here is of the right order of magnitude. Harris & Hutter (1956) found that the rate of movement of potassium ions in the sinus venosus may be increased two to three times by acetylcholine; the conductance increase assumed in Fig. 13 is approximately twofold at the resting potential.

Like the plateau, the pace-maker potential is very sensitive to changes in ionic permeability. Thus, an increase in g_K by only 0·1 mmho/cm² is sufficient to stop pace-maker activity completely in these equations. In this respect the equations mimic the behaviour of the natural pace-maker when g_K is increased by vagal stimulation (Hutter & Trautwein, 1956).

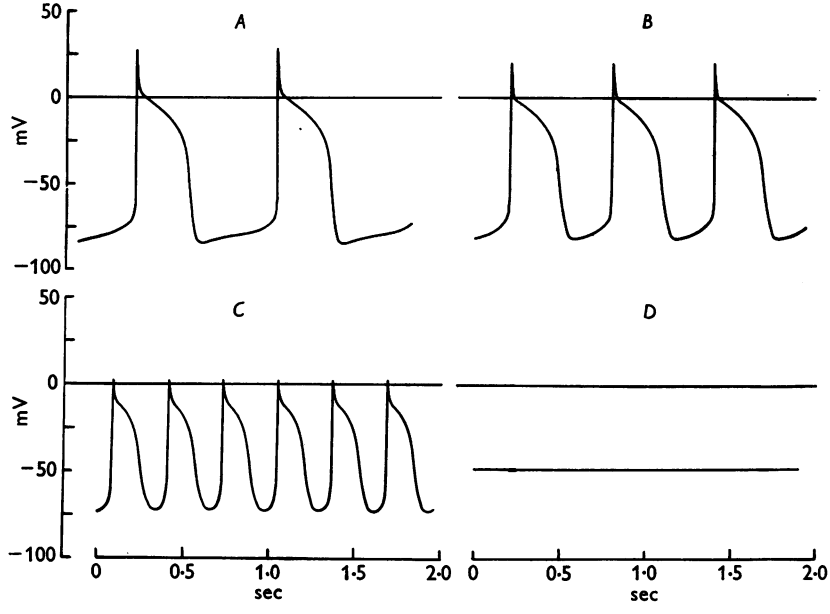

Fig. 14. Effect of various anion conductances on the computed pacemaker potential. *A*, $g_{An} = 0$; *B*, $g_{An} = 0{\cdot}075$ mmho/cm²; *C*, $g_{An} = 0{\cdot}18$ mmho/cm²; *D*, $g_{An} = 0{\cdot}4$ mmho/cm². $E_{An} = -60$ mV in all cases. Description in text.

Rather striking alterations in pace-maker activity are observed when different anions are present in the extracellular fluid (Hutter & Noble, 1961) and these may also be reproduced by the equations. It seems likely that in continuously active fibres the anion equilibrium potential is low (Hutter & Noble, 1961) and E_{An} was therefore set at -60 mV. The results of inserting this value for E_{An} and various values for g_{An} are shown in Fig. 14. Curve *A* shows the solution obtained when $g_{An} = 0$ and is the same as that in Fig. 6*A*. When g_{An} is increased to 0·075 mmho/cm²

(curve B) the frequency increases by about 50% while the shape and duration of the action potential are only slightly affected. This resembles the effect of Cl ions on Purkinje fibres.

When g_{An} is increased to 0·18 mmho/cm^2 (curve C) the frequency greatly increases, the maximum diastolic potential falls, the action potential is markedly shortened and the overshoot is almost completely abolished. This closely resembles the effect of prolonged exposure to NO_3 ions on spontaneously beating Purkinje fibres. The value of g_{An} assumed in Fig. 14 is almost equal to that assumed in order to reproduce the effect of NO_3 ions on a driven fibre (Fig. 13). Thus, in so far as the relative sensitivity of the plateau and pace-maker potential to changes in anion conductance is concerned the behaviour of the equations is consistent.

A further increase in g_{An} to 0·4 mmho/cm^2 (curve D) does not produce an increase in frequency but has the effect of arresting the 'fibre'. This effect is obtained in Purkinje fibres when Cl ions are replaced by I ions (Hutter & Noble, 1961).

The dual effect which a progressive increase in g_{An} has on the computed pace-maker may appear surprising, since only one factor in the equations is being varied. The explanation lies in the fact that E_{An} is assumed to be considerably less negative than E_K. A moderate increase in g_{An} accelerates the depolarization towards E_{An} during diastole and so increases the frequency. A large enough increase in g_{An}, however, stabilizes the potential at or near E_{An}, so that pace-maker activity is completely abolished.

DISCUSSION

Discrepancies between computed and recorded action potentials

So far as the potential changes are concerned the main discrepancy is that the maximum rate of depolarization, $dE_m/dt_{max.}$, during the spike is much smaller in the computed action potentials than in those recorded experimentally. This difference cannot be attributed to progressive errors in the computation, as the same result was obtained when the integration was repeated at shorter step lengths. Nor can it be attributed to the fact that the recorded action potentials were propagating, since initially, when d^2E_m/dt^2 is positive, current would be drawn away from the membrane and so reduce the current discharging the membrane capacity. This would slow the rate of depolarization and allow more time for h to fall, so that when $dE_m/dt_{max.}$ is reached, g_{Na} would be smaller in the propagating action potential than in the membrane action potential. Thus, in squid nerve the computed values for $dE_m/dt_{max.}$ are 431 V/sec for a propagated action potential and 564 V/sec for a membrane action potential (Hodgkin & Huxley, 1952*d*).

There remain two other possibilities. First, the computed maximum depolarizing current may be too small. This would appear to be a very likely error in view of the somewhat arbitrary way in which the equations for m were obtained (see Methods). It is difficult, however, to see how such an error might be rectified without radically affecting the other phases of the action potential. In order for I_{Na} to be increased at a given E_m, either $\bar{g}_{Na}$ or m or both must be increased, but this would have the effect of greatly prolonging the plateau or of preventing repolarization altogether (see Fig. 4). Furthermore, the computed increase in membrane conductance during the spike is in good agreement with that observed by Weidmann. It seems unlikely, therefore, that the peak sodium current is seriously underestimated by the equations.

The other possibility is that only a small part of the membrane capacity is discharged during the spike of the action potential. This would happen if the major part of the capacity were to be in series with a resistance which is small compared to the resting membrane resistance but fairly large compared to the membrane resistance during the spike. This part of the capacity would then be discharged mainly during the beginning of the plateau. If 10 μF/cm^2 were to be discharged slowly in this way, this would leave only 2 μF/cm^2 to be discharged by the sodium current during the spike and $dE_m/dt_{max.}$ would be increased by about the required factor. In physical terms this might mean that a large fraction of the membrane capacity is distributed along invaginated folds or tubules of membrane, the series resistance being the resistance of the 'extracellular' fluid in the folds or tubules. In the case of skeletal muscle the existence of intracellular tubules of membrane has been clearly demonstrated in observations made with the electron microscope (Bennett & Porter, 1953; Edwards & Ruska, 1955; Robertson, 1956; Porter & Palade, 1957) and Huxley & Taylor (1958) have shown that it is very likely that some process like spread of depolarization occurs along these tubules. At present, however, there is no direct evidence to support the idea that the tubules open out on the fibre surface (Huxley, 1959*b*), though this is not essential, provided that there is electrical continuity via a low resistance between the tubular fluid and the extracellular fluid, as suggested by Hodgkin & Horowicz (1960). Fatt (1961) has shown that the high-frequency membrane capacity of frog skeletal muscle is about 2 μF/cm^2, which may be compared with the value of 6–8 μF/cm^2 obtained with 'square-wave' current analysis using intracellular micro-electrodes (Fatt & Katz, 1951). The situation in Purkinje fibres has not yet been investigated and another possibility which cannot be ruled out is that part of the capacitative behaviour observed in the resting fibre may be anomalous, in that it may result from delayed voltage-dependent changes in permeability. This would

be analogous, though opposite, to the anomalous inductive behaviour resulting from delayed K rectification in squid nerve.

Another difference between the computed and experimentally recorded curves is that the rate of fall of E_m from the peak of the spike to the plateau is smaller in the computed action potential. This might also be explained by assuming a smaller capacity during the spike. On the other hand, dE_m/dt here greatly depends on g_K and would be appreciably larger if g_{K_1} were not to fall instantaneously on depolarization of the membrane, but rather with a small delay. Such a delay might also account for the 'notch' often observed between the spike and plateau of the Purkinje fibre action potential (Draper & Weidmann, 1951, Fig. 4*b*).

Ionic fluxes in cardiac muscle

At present there is very little information available on the effect of activity on the Na fluxes in cardiac muscle, so that it is not yet possible to say how far the computed fluxes correspond to those actually occurring. In the case of potassium, experiments on different specie shave given different results. Brady (unpublished, quoted by Brady & Woodbury, 1960) found no increase in K efflux during activity in the frog ventricle. This result is consistent with the theory given here, as it is also with that given by Brady & Woodbury (1960). Wilde & O'Brien (1953) found an increase in K efflux in the turtle ventricle which they considered to be synchronous with the action potential. Weidmann (1956) has calculated that the potential changes during the action potential are themselves sufficient to account for Wilde & O'Brien's results, so that there is no need to suppose that g_K increases during the action potential. One possibility, therefore, is that potassium rectification does not occur at all in this preparation. It is difficult, however, to reconcile this suggestion with the fact that the resistance during the plateau of the turtle ventricle action potential is greater than the resting resistance (Eyster & Gilson, 1947; Cranefield, Eyster & Gilson, 1951). This observation is readily explained by supposing that g_K is reduced during the action potential (see Fig. 10). A dependence of g_K on the K electrochemical potential gradient will also explain the shortening of the turtle heart action potential produced by increasing the extracellular potassium concentration (Weidmann, 1956*a*; cf. Hoffmann & Cranefield, 1960). It does not therefore seem possible at present to reconcile Wilde & O'Brien's results with those of electrical experiments.

Comparison of theories concerning long-lasting action potentials

Various modifications of Hodgkin & Huxley's original equations have been suggested recently in order to account for long-lasting action

potentials, and it seems desirable briefly to summarize and compare their main features.

The modification proposed by Fitzhugh (1960) and the closely similar one of George & Johnson (1961) primarily involve a large decrease in the rate constants of the potassium current system (α_n and β_n). g_K increases on depolarization of the membrane but does so very much more slowly than in normal squid nerve. For the purpose of describing the properties of cardiac muscle this modification is not sufficient, as it does not account for the high resistance during the plateau of the action potential which has been observed in kid Purkinje fibres (Weidmann, 1951), turtle ventricle fibres (Eyster & Gilson, 1947; Cranefield *et al.* 1951) and rabbit ventricular fibres (Johnson & Tille, 1960). Thus in Fitzhugh's computations the resistance during the plateau is only about one-quarter of the resting resistance, while in cardiac muscle the plateau resistance is as great or even greater than the resting resistance. On the basis of this difference it has been suggested (e.g. Chang & Schmidt, 1960) that the Hodgkin–Huxley formulation is inadequate to account for the electrical properties of cardiac muscle and that other models such as the two-stable state hypothesis (Tasaki & Hagiwara, 1957) might be more applicable. So far as its essential features are concerned the differences between this hypothesis and that of Hodgkin & Huxley are not very great. As Fitzhugh (1960) has pointed out, Tasaki & Hagiwara's description of the transition from one stable to the other at the termination of the plateau is a good qualitative description of the way in which the modified Hodgkin–Huxley equations actually behave, and the objection based on the discrepancies between observed and computed resistance changes does not apply to the equations used in this paper (see Fig. 10).

Brady & Woodbury (1960) have recently formulated equations to describe the action potential in frog ventricle. They postulated that the principal differences between cardiac muscle and squid nerve are: (1) that g_K falls on depolarization of the cardiac fibre membrane, and (2) that the Na inactivation and activation processes in heart muscle have two components, a slow one (time constant of the order of seconds) and a fast one (time constant of the order of milliseconds, as in squid nerve). Although their equations adequately describe the frog ventricle action potential and its main properties, including Brady's failure to observe any increase of K efflux associated with activity, they had no direct experimental evidence for the modifications which they proposed. So far as Purkinje fibres are concerned, the presence of a slow component in the Na inactivation process would seem unlikely in view of Weidmann's (1955) experiments.

In the equations used in this paper the main modification involves the K current which is assumed to flow through two types of channel in the

membrane, one in which g_K falls on depolarization of the membrane and another in which g_K slowly rises (Noble 1960*a*, *b*). This hypothesis was suggested by Hutter & Noble's (1960) experiments on Purkinje fibres in Na-deficient solutions. The modification made to the Na equations is a minor one, in that it does not involve any qualitative change in the behaviour of the sodium current system, but it is necessary in order that the equations should describe the action potential shape accurately. The h equations have been unaltered, apart from the shift along the voltage axis required to make the equations fit Weidmann's (1955) experimental curve, but the m equations have been reformulated in order to make the m_∞/E_m relation less steep than that of Hodgkin & Huxley (see Figs. 4 and 5).

The result of using the Hodgkin–Huxley m equations would be greatly to lower the position of the plateau and to decrease the magnitude of the maximum diastolic potential. This is illustrated in Fig. 15. The interrupted curves are the instantaneous K current–voltage relations shown in Fig. 9, and the thin continuous curve is the steady-state Na current–voltage relation given by the Na equations used in this paper. The thick continuous curve is a steady-state Na relation obtained by substituting Hodgkin & Huxley's m equations (equations (24) and (25)) and by setting $\bar{g}_{Na}$ at 30 mmho/cm^2, and the fraction of g_{Na} which is assumed to be independent of E_m and t at 0·25 mmho/cm^2. The peak value of the steady-state Na current now occurs at a more negative potential and the value of $\bar{g}_{Na}$ has been reduced in order that the steady-state Na current should not exceed the steady-state K current at this potential. Without integrating the equations it is clear from Fig. 15 that normal Purkinje fibre-like action and pace-maker potentials would not be obtained. The low value required for $\bar{g}_{Na}$, and the fact that the action potential would start at a potential (about -65 mV) at which h is small, mean that the rate of rise would be greatly reduced and there would be no initial spike or overshoot. The plateau would start at about -25 mV and terminate at about -45 mV. The point of maximum repolarization would be at about -75 mV.

The ability of the equations used in this paper to describe the shape of the action and pace-maker potentials fairly accurately is to a great extent due to the fact that the action potential itself was used as a source of information in obtaining the equations for m (see Methods). However, the equations also account for most of the other electrical properties of Purkinje fibres, including the impedance changes, the responses to applied current pulses, the effect of repetitive stimulation and the influence of changes in ionic permeability, which were not used in formulating the equations. Nevertheless, they are not yet based on sufficient direct experimental evidence and will probably require further detailed modification

when the results of voltage-clamp analysis similar to that done in squid nerve are known.

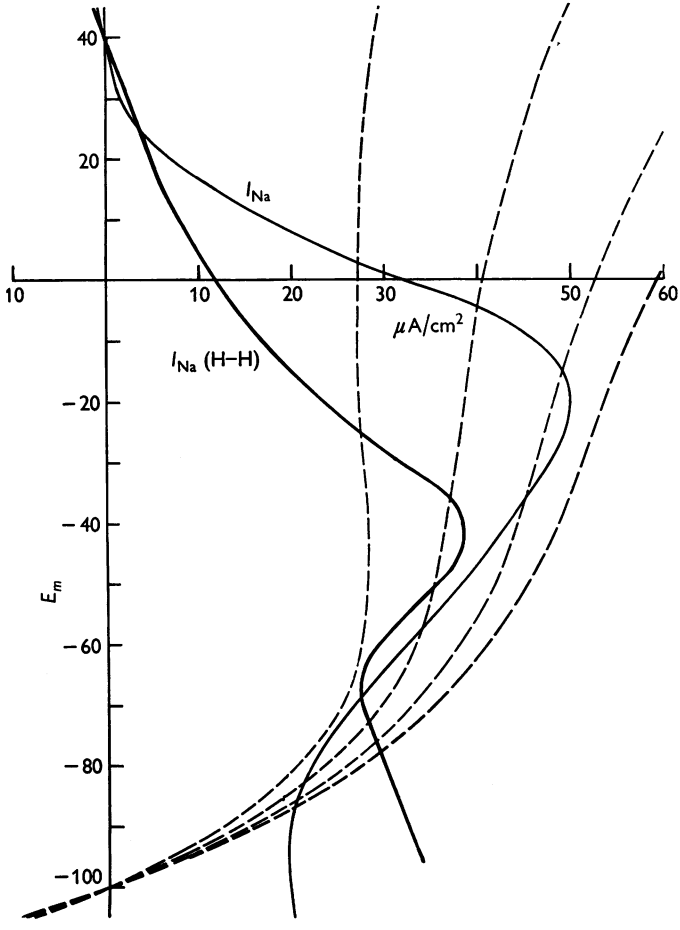

Fig. 15. Ionic current–voltage relations. Interrupted curves, instantaneous K current–voltage relations at various stages during computed action potential—same curves as in Fig. 9. Thin continuous curve, steady-state Na current–voltage relation given by Na equations used in this paper (as in Fig. 9). Thick continuous curve, Na current–voltage relation obtained by substituting Hodgkin & Huxley's m equations. Explanation in text.

SUMMARY

1. The equations formulated by Hodgkin & Huxley (1952*a*, *b*, *c*, *d*) to describe the electrical activity of squid nerve have been modified to describe the action and pace-maker potentials of the Purkinje fibres of the heart.

2. The potassium-current equations differ from those of Hodgkin & Huxley in that K ions are assumed to flow through two types of channel in the membrane: one in which g_K falls when the membrane is depolarized and another in which g_K very slowly rises.

3. The sodium-current equations are very similar to those of Hodgkin & Huxley and are in part based on Weidmann's (1955) measurements of the properties of the h system in cardiac muscle. A method for obtaining equations for m by using some features of the action potential as an additional source of information is described.

4. The solution to these equations closely resembles the potential changes in Purkinje fibres, the only major discrepancy being that the maximum rate of depolarization is smaller in the computed action potentials than in those recorded experimentally. Possible reasons for this discrepancy are discussed.

5. The predicted changes in ionic conductances, ionic currents and fluxes are described.

6. The variation in the computed membrane impedance during the action and pace-maker potentials is very similar to that observed experimentally in Purkinje fibres.

7. Some of the effects of applied currents, repetitive stimulation and changes in ionic permeabilities have been reproduced. In general, the behaviour of the equations corresponds quite well with the observed behaviour of Purkinje fibres.

I should like to thank Professor A. F. Huxley for his comments on the manuscript of this paper, and Drs O. F. Hutter, R. Niedergerke and S. J. Hubbard for valuable discussion. I am also grateful to Dr R. A. Buckingham, Director of the University of London Computer Unit, for permission to use 'Mercury' and to Dr M. J. M. Bernal and other members of the Computer Unit Staff for advice on writing the programmes.

This work has been submitted in part fulfilment of the requirements for the degree of Ph.D. at London University.

REFERENCES

BENNETT, H. S. & PORTER, K. R. (1953). An electron microscope study of sectioned breast muscle of the domestic fowl. *Amer. J. Anat.* **93**, 61–105.

BRADY, A. J. & WOODBURY, J. W. (1960). The sodium–potassium hypothesis as the basis of electrical activity in frog ventricle. *J. Physiol.* **154**, 385–407.

CARMELIET, E. (1955*a*). Influence du rhythme sur la durée du potentiel d'action ventriculaire cardiaque. *Arch. int. Physiol.* **63**, 126–127.

CARMELIET, E. (1955*b*). Influence du rhythme sur la durée du potentiel d'action ventriculaire cardiaque. *Arch. int. Physiol.* **63**, 222–232.

CARMELIET, E. (1961). Chloride ions and the membrane potential of Purkinje fibres. *J. Physiol.* **156**, 375–388.

CARR, J. W. (1958). Error bounds for the Runge–Kutta single-step integration process. *J. Ass. comp. Mach.* **5**, 39–44.

CHANG, J. J. & SCHMIDT, R. F. (1960). Prolonged action potentials and regenerative repolarizing responses in Purkinje fibres of mammalian heart. *Pflüg. Arch. ges. Physiol.* **272**, 127–141.

COLE, K. S., ANTOSIEWICZ, H. A. & RABINOWITZ, P. (1955). Automatic computation of nerve excitation. *J. Soc. indust. appl. Math.* **3**, 135–172.

COLE, K. S. & CURTIS, H. J. (1941). Membrane potential of the squid giant axon during current flow. *J. gen. Physiol.* **24**, 551–563.

CORABOEUF, E. & WEIDMANN, S. (1954). Temperature effects on the electrical activity of Purkinje fibres. *Helv. physiol. acta*, **12**, 32–41.

CRANEFIELD, P. F., EYSTER, J. A. E. & GILSON, W. E. (1951). Electrical characteristics of injury potentials. *Amer. J. Physiol.* **167**, 450–456.

CURTIS, H. J. & COLE, K. S. (1940). Membrane action potentials from the squid giant axon. *J. cell. comp. Physiol.* **15**, 147–157.

CURTIS, H. J. & COLE, K. S. (1942). Membrane resting and action potentials from the squid giant axon. *J. cell. comp. Physiol.* **19**, 135–144.

DRAPER, M. H. & WEIDMANN, S. (1951). Cardiac resting and action potentials recorded with an intracellular electrode. *J. Physiol.* **115**, 74–94.

EDWARDS, G. A. & RUSKA, H. (1955). The function and metabolism of certain insect muscles in relation to their structures. *Quart. J. micr. Sci.* **96**, 151–159.

EYSTER, J. A. E. & GILSON, W. E. (1947). Electrical characteristics of injuries to heart muscle. *Amer. J. Physiol.* **150**, 572–579.

FATT, P. (1961). Transverse impedance measurements of striated muscles. *J. Physiol.* **157**, 10–12*P*.

FATT, P. & KATZ, B. (1951). An analysis of the end-plate potential recorded with an intracellular electrode. *J. Physiol.* **115**, 320–370.

FITZHUGH, R. (1960). Thresholds and plateaus in the Hodgkin–Huxley nerve equations. *J. gen. Physiol.* **43**, 867–896.

FRANKENHAEUSER, B. & HODGKIN, A. L. (1957). The action of calcium on the electrical properties of squid axons. *J. Physiol.* **137**, 218–244.

GEORGE, E. P. & JOHNSON, E. A. (1961). Solutions of the Hodgkin–Huxley equations for squid axon treated with tetraethylammonium and in potassium rich media. *Aust. J. exp. biol. Sci.* (in the Press).

HARRIS, E. J. & HUTTER, O. F. (1956). The action of acetylcholine on the movements of potassium ions in the sinus venosus of the heart. *J. Physiol.* **133**, 58–59*P*.

HODGKIN, A. L. & HOROWICZ, P. (1960). The effect of sudden changes in ionic concentration on the membrane potential of single muscle fibres. *J. Physiol.* **153**, 370–385.

HODGKIN, A. L. & HUXLEY, A. F. (1939). Action potentials recorded from inside a nerve fibre. *Nature, Lond.*, **144**, 710.

HODGKIN, A. L. & HUXLEY, A. F. (1945). Resting and action potentials in single nerve fibres. *J. Physiol.* **104**, 176–195.

HODGKIN, A. L. & HUXLEY, A. F. (1952*a*). Currents carried by sodium and potassium ions through the membrane of the giant axon of *Loligo*. *J. Physiol.* **116**, 449–472.

HODGKIN, A. L. & HUXLEY, A. F. (1952*b*). The components of membrane conductance in the giant axon of *Loligo*. *J. Physiol.* **116**, 473–496.

HODGKIN, A. L. & HUXLEY, A. F. (1952*c*). The dual effect of membrane potential on sodium conductance in the giant axon of *Loligo*. *J. Physiol.* **116**, 497–506.

HODGKIN, A. L. & HUXLEY, A. F. (1952*d*). A quantitative description of membrane current and its application to conduction and excitation in nerve. *J. Physiol.* **117**, 500–544.

HODGKIN, A. L., HUXLEY, A. F. & KATZ, B. (1949). Ionic currents underlying activity in the giant axon of the squid. *Arch. Sci. physiol.* **3**, 129–150.

HODGKIN, A. L. & KATZ, B. (1949). The effect of sodium ions on the electrical activity of the giant axon of the squid. *J. Physiol.* **108**, 37–77.

HOFFMANN, B. F. & CRANEFIELD, P. F. (1960). *Electrophysiology of the Heart.* New York: McGraw-Hill Book Company.

HOFFMANN, B. F. & SUCKLING, E. E. (1954). Effects of heart rate on cardiac membrane potentials and the unipolar electrogram. *Amer. J. Physiol.* **179**, 123–130.

HUTTER, O. F. & NOBLE, D. (1960). Rectifying properties of cardiac muscle. *Nature, Lond.*, **188**, 495.

HUTTER, O. F. & NOBLE, D. (1961). Anion conductance of cardiac muscle. *J. Physiol.* **157**, 335–350.

HUTTER, O. F. & TRAUTWEIN, W. (1956). Vagal and sympathetic effects on the pacemaker fibres in the sinus venosus of the heart. *J. gen. Physiol.* **39**, 715–733.

HUXLEY, A. F. (1959*a*). Ion movements during nerve activity. *Ann. N.Y. Acad. Sci.* **81**, 221–246.

HUXLEY, A. F. (1959*b*). Local activation of muscle. *Ann. N.Y. Acad. Sci.* **81**, 446–452.

HUXLEY, A. F. & TAYLOR, R. E. (1958). Local activation of striated muscle fibres. *J. Physiol.* **144**, 426–441.

JOHNSON, E. A. & TILLE, J. (1960). Changes in polarization resistance during the repolarization phase of the rabbit ventricular action potential. *Aust. J. exp. biol. Sci.* **58**, 509–513.

KEYNES, R. D. (1951). The ionic movements during nervous activity. *J. Physiol.* **114**, 119–150.

NATIONAL PHYSICAL LABORATORY (1961). *Modern Computing Methods*, 2nd ed., p. 90. London: H.M.S.O.

MOORE, J. W. (1959). Squid action potentials in isosmotic KCl. *Fed. Proc.* **18**, 107.

NOBLE, D. (1960*a*). Cardiac action and pacemaker potentials based on the Hodgkin–Huxley equations. *Nature, Lond.*, **188**, 495–497.

NOBLE, D. (1960*b*). A description of cardiac pace-maker potentials based on the Hodgkin–Huxley equations. *J. Physiol.* **154**, 64–65*P*.

NOBLE, D. (1961). Ionic conductance of cardiac muscle. Ph.D. Thesis. University of London.

PORTER, K. R. & PALADE, G. E. (1957). Studies on the endoplasmic reticulum. III. Its form and distribution in striated muscles. *J. biophys. biochem. Cytol.* **3**, 269–300.

ROBERTSON, J. D. (1956). Some features of the ultrastructure of reptilian skeletal muscle. *J. biophys. biochem. Cytol.* **2**, 369–380.

SCHÜTZ, E. (1936). Elektrophysiologie der Herzens bei einphasischer Ableitung. *Ergebn. Physiol.* **38**, 493–620.

SEGAL, J. R. (1958). An anodal threshold phenomenon in the squid giant axon. *Nature, Lond.*, **182**, 1370–1372.

TASAKI, I. (1959). Demonstration of two stable states of the nerve membrane in potassium-rich media. *J. Physiol.* **148**, 306–331.

TASAKI, I. & HAGIWARA, S. (1957). Demonstration of the stable potential states in the squid giant axon under tetraethylammonium chloride. *J. gen. Physiol.* **40**, 859–885.

TRAUTWEIN, W. & DUDEL, J. (1954). Aktionspotential und Mechanogramm des Warmblüterherzmuskels als Funktion der Schlagfreqenz. *Pflüg. Arch. ges. Physiol.* **260**, 24–39.

TRAUTWEIN, W., GOTTSTEIN, U. & FEDERSCHMIDT, K. (1953). Der Einfluss der Temperatur auf den Aktionsstrom des excidierten Purkinje-fadens, gemessen mit einer intracellularen Elektrode. *Pflüg. Arch. ges. Physiol.* **258**, 243–360.

WEIDMANN, S. (1951). Effect of current flow on the membrane potential of cardiac muscle. *J. Physiol.* **115**, 227–236.

WEIDMANN, S. (1952). The electrical constants of Purkinje fibres. *J. Physiol.* **118**, 348–360.

WEIDMANN, S. (1955). The effect of the cardiac membrane potential on the rapid availability of the sodium carrying system. *J. Physiol.* **127**, 213–224.

WEIDMANN, S. (1956*a*). Shortening of the cardiac action potential due to a brief injection of KCl following the onset of activity. *J. Physiol.* **132**, 157–163.

WEIDMANN, S. (1956*b*). *Elektrophysiologie der Herzmuskelfaser*. Bern: Huber.

WILDE, W. S. & O'BRIEN, J. M. (1953). The time relation between potassium (K^{42}) outflux, action potential, and the contraction phase of heart muscle as revealed by the effluogram. *Abstr. XIX int. physiol. Congr.* pp. 889–890.